Bidirectional plasticity in the primate inferior olive induced by chronic ethanol intoxication and sustained abstinence

John P. Welsh[a,b,1], Victor Z. Han[a], David J. Rossi[c], Claudia Mohr[c], Misa Odagiri[d], James B. Daunais[e], and Kathleen A. Grant[c,d,1]

[a]Center for Integrative Brain Research, Seattle Children's Research Institute, Seattle, WA 98101; [b]Department of Pediatrics, University of Washington, Seattle, WA 98195; [c]Department of Behavioral Neuroscience, Oregon Health Science University, Portland, OR 97239; [d]Division of Neuroscience, Oregon National Primate Research Center, Beaverton, OR 97006; and [e]Department of Physiology and Pharmacology, Wake Forest School of Medicine, Winston-Salem, NC 27157

Edited* by Rodolfo R. Llinas, New York University Medical Center, New York, NY, and approved May 4, 2011 (received for review November 12, 2010)

The brain adapts to chronic ethanol intoxication by altering synaptic and ion-channel function to increase excitability, a homeostatic counterbalance to inhibition by alcohol. Delirium tremens occurs when those adaptations are unmasked during withdrawal, but little is known about whether the primate brain returns to normal with repeated bouts of ethanol abuse and abstinence. Here, we show a form of bidirectional plasticity of pacemaking currents induced by chronic heavy drinking within the inferior olive of cynomolgus monkeys. Intracellular recordings of inferior olive neurons demonstrated that ethanol inhibited the tail current triggered by release from hyperpolarization (I_{tail}). Both the slow deactivation of hyperpolarization-activated cyclic nucleotide-gated channels conducting the hyperpolarization-activated inward current and the activation of $Ca_V3.1$ channels conducting the T-type calcium current (I_T) contributed to I_{tail}, but ethanol inhibited only the I_T component of I_{tail}. Recordings of inferior olive neurons obtained from chronically intoxicated monkeys revealed a significant up-regulation in I_{tail} that was induced by 1 y of daily ethanol self-administration. The up-regulation was caused by a specific increase in I_T which (*i*) greatly increased neurons' susceptibility for rebound excitation following hyperpolarization and (*ii*) may have accounted for intention tremors observed during ethanol withdrawal. In another set of monkeys, sustained abstinence produced the opposite effects: (*i*) a reduction in rebound excitability and (*ii*) a down-regulation of I_{tail} caused by the down-regulation of both the hyperpolarization-activated inward current and I_T. Bidirectional plasticity of two hyperpolarization-sensitive currents following chronic ethanol abuse and abstinence may underlie persistent brain dysfunction in primates and be a target for therapy.

Acute ethanol withdrawal affects millions of people and can require management of a syndrome that consists of dysautonomia, seizures, cognitive disturbance, and tremor (1, 2). It generally is agreed that the washout of ethanol from the brain during acute withdrawal unmasks the physiological adaptations of neurons that allow them to function while they are bathed in ethanol (3, 4). It sometimes is assumed that once the symptoms of acute withdrawal are managed, long-term abstinence from ethanol gradually restores the brain to a preethanol state. Nevertheless, an alcoholic's drive to ingest ethanol can persist even after months or years of abstinence, and alcoholics can undergo multiple abstinences from alcohol in their lifetime.

We tested the hypothesis that adaptations in the intrinsic electrical properties of inferior olive (IO) neurons are changed by chronic ethanol intake and by subsequent abstinence. We used patch-clamp recordings of IO neurons in acutely prepared brainstem slices from chronically intoxicated cynomolgus monkeys (5–7) to examine changes in intrinsic electrical properties with ethanol intake and repeated abstinences. We addressed two questions: (*i*) Does acute washout of ethanol from the brain of a primate with an alcoholic drinking phenotype produce withdrawal behaviors and unmask an up-regulation in pacemaking T-type calcium (I_T) and hyperpolarization-activated inward (I_h) currents in the IO, and, if so, (*ii*) do the behaviors and intrinsic electrical properties of neurons of alcoholic primates return to their preethanol state after sustained abstinences?

The IO is a cerebellar afferent involved in movement control (8, 9) that has been implicated in generating non-Parkinsonian tremors such as physiological tremor and essential tremor (10) and perhaps alcohol withdrawal tremor (11). The link between the IO and tremor was made first on the basis of studies demonstrating electrical pacemaking in IO neurons (12–14), which produced tremor when activated with β-carbolines (15, 16). Electrical pacemaking in IO neurons is mediated primarily by $Ca_V3.1$ calcium channels that conduct I_T, generate 5- to 10-Hz oscillations in membrane potential that entrain spikes (14, 17), and trigger rebound firing from a hyperpolarized membrane potential (12, 13). In addition, hyperpolarization-activated cyclic nucleotide-gated (HCN) channels that conduct I_h also facilitate rebound firing in IO neurons (18). In rodents, I_T was inhibited acutely by ethanol and long-chain aliphatic alcohols (19, 20), whereas I_h was augmented by ethanol (21). Recent studies demonstrated that the tremor mediated by the IO requires $Ca_V3.1$ T-type calcium channels (22, 23) and is synchronized by gap junctions (24).

Here, we demonstrate that primate IO neurons are oscillatory pacemakers and that chronic intoxication for over 1 y in monkeys is associated with potentiated $Ca_V3.1$ channel function within the IO and acute withdrawal tremor. Our experiments indicate that sustained (30-d) abstinence following chronic intoxication does not return the brain to the preethanol state but rather is associated with a below-normal decrease in rebound excitability in IO neurons and therefore reveals a form of bidirectional plasticity of pacemaking excitability.

Results

Ethanol Self-Administration and Alcoholism Phenotype. Fig. 1*A* shows the experimental timeline for 22 cynomolgus monkeys (*Macaca fascicularis*). The monkeys were divided into two groups that did ($n = 11$; six males and five females) or did not ($n = 11$; nine males and two females) drink ethanol. The monkeys that did not drink ethanol were termed the "control" (CON) group and consisted of monkeys that drank water ad libitum for 34 mo (CONa; $n = 6$ males) or were treated identically to the experimental groups for 16 mo except that they drank maltose-dextrose solution instead of ethanol (CONb; $n = 5$; three males

Author contributions: J.P.W., D.J.R., J.B.D., and K.A.G. designed research; J.P.W., V.Z.H., D.J.R., C.M., M.O., J.B.D., and K.A.G. performed research; J.P.W., V.Z.H., D.J.R., and K.A.G. analyzed data; and J.P.W., D.J.R., and K.A.G. wrote the paper.

The authors declare no conflict of interest.

*This Direct Submission article had a prearranged editor.

Freely available online through the PNAS open access option.

[1]To whom correspondence may be addressed. E-mail: john.welsh@seattlechildrens.org or grantka@ohsu.edu.

This article contains supporting information online at www.pnas.org/lookup/suppl/doi:10.1073/pnas.1017079108/-/DCSupplemental.

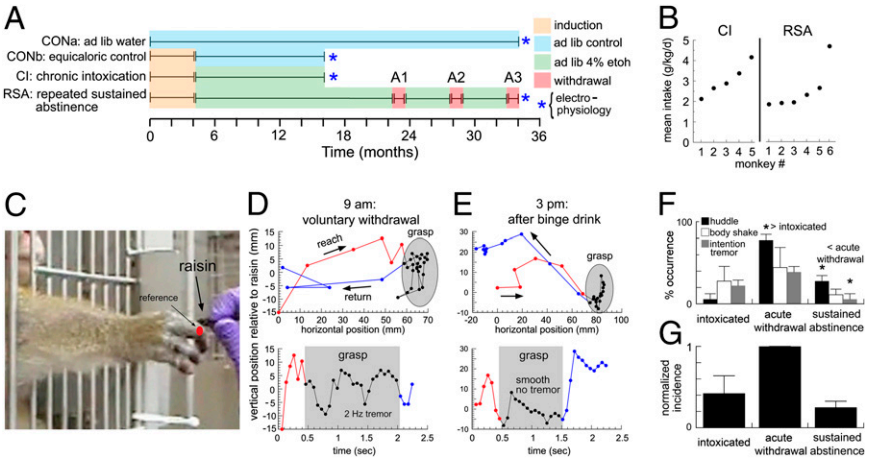

Fig. 1. Alcoholic phenotype in cynomolgus monkeys. (*A*) Experimental timeline. (*B*) Mean ethanol intake for five CI monkeys in the month before necropsy and for six RSA monkeys during the 4 mo before their last withdrawal. (*C*) Reach-to-grasp task. The third metacarpophalangeal joint (red) was used to reference hand trajectory. (*D*) Plots of the reach (red), grasp (black), and return (blue) phases after a day of voluntary withdrawal (Fig. S1*A*) as spatial trajectories (*Upper*) and vertical position over time (*Lower*). (*E*) As in *D* but after a drinking binge. (*F*) Occurrence of three behaviors during intoxication, acute withdrawal, and sustained abstinence for RSA monkeys. $*P < 0.05$. (*G*) Normalized incidence of alcohol-withdrawal behaviors.

and two females). No differences were observed between neurons obtained from CONa and CONb monkeys, and they were pooled. The 11 ethanol-drinking monkeys were induced to drink 4% (wt/vol) ethanol over 4 mo (5–7) and self-administered ethanol, with a concurrent choice of water, for 22 h/d access for 1 y. Thereafter, the history of the monkeys diverged. The first subgroup was termed the "chronic intoxication" (CI) subgroup ($n = 5$). CI monkeys were killed for necropsy; their brains were removed and prepared for electrophysiology (i.e., washed of ethanol) on the morning of what would have been a typical day of drinking. The second subgroup was termed the "repeated sustained abstinence" (RSA) group ($n = 6$). RSA monkeys self-administered ethanol for 1.5 y and then experienced three 28-d periods of ethanol abstinence separated by two 4-mo periods of ethanol access. The RSA paradigm provided an examination of the consequences of repeated bouts of ethanol abstinence and relapse with highly controlled timing. The brains of RSA monkeys were prepared for electrophysiology on the morning of the 30th day of the last abstinence period.

During 12 mo of free access, the ethanol intake of CI monkeys was 3.11 ± 0.43 $g{\cdot}kg^{-1}{\cdot}d^{-1}$ [range 1.88–3.93 $g{\cdot}kg^{-1}{\cdot}d^{-1}$; 46–140 mg/dL blood ethanol concentration (BEC)], and intake during the last month averaged 3.04 ± 0.36 $g{\cdot}kg^{-1}{\cdot}d^{-1}$ (Fig. 1*B*). The intake of RSA monkeys was 2.57 ± 0.47 $g{\cdot}kg^{-1}{\cdot}d^{-1}$during the month before the last abstinence period (range 1.94–4.67 $g{\cdot}kg^{-1}{\cdot}d^{-1}$; 61–266 mg/dL BEC; Fig. 1*B*).

The behavior of CI and RSA monkeys modeled two features of human alcoholism: highly regulated intake and acute withdrawal tremor. Regulated intake was acquired by nearly all monkeys and was exemplified by the heaviest-drinking monkey (Fig. S1*A*). For this monkey, mean monthly intake deviated from the annual mean by only 6.8 ± 0.7%. However, there was a significant change in the day-to-day variation (Fig. S1*B*). Daily intake was highly variable during the first 200 d of self-administration, varying from the annual mean by 79.7 ± 20.5%. Later, daily intake became regulated and varied from the annual mean by only 25.1 ± 11.3% [$t(335) = 2.07$; $P < 0.05$], modeling the narrow drinking repertoires of alcoholic humans (1).

In the course of observing the monkey, whose drinking record is shown in Fig. S1, it was noticed that the monkey lowered its intake from 4.39 to 0.28 g/kg on a single day after 138 d of high intake (arrow in Fig. S1*A*). Early the following morning, staff reported that the monkey was in a state of withdrawal and showed "wet-dog" body shakes, huddling, and postural tremor. To quantify the tremor, we tested the monkey in a reach-to-grasp task (Fig. 1*C*) while recording its movement by video (Fig. 1 *D* and *E*). During acute withdrawal, the monkey's hand demonstrated a prominent 15-mm, 2-Hz tremor during the grasp phase of the reach (Fig. 1*D Lower*). When retested after binge drinking for 6 h (2.78 g/kg/6 h), the hand showed a smooth downward trajectory during the grasp (Fig. 1*E Upper*) without tremor (Fig. 1*E Lower*). The morning tremor after a day of abstinence and its reduction with later drinking was consistent with ethanol withdrawal tremor (25). That event motivated a systematic study of the six monkeys during the abstinence phases of the RSA paradigm. The morning occurrence of body shaking, huddling, and reaching tremor was noted during intoxication, the first 72 h of abstinence (acute withdrawal), and at 18–22 d of sustained abstinence. The incidence of all three behaviors was highest during acute withdrawal and reversed with abstinence (Fig. 1 *F* and *G*), suggesting a bidirectional adaptive process.

Primate IO Neurons Are Oscillatory with Pacemaking I_h and I_T. Current- and voltage-clamp recordings were obtained from 53 IO neurons taken from CON monkeys. The IO was easily identifiable from the external brainstem anatomy (Fig. 2*A*). As previously reported for guinea pig (14), rat (17, 26), mouse (27, 28), and ferret (18), primate IO neurons demonstrated oscillations in

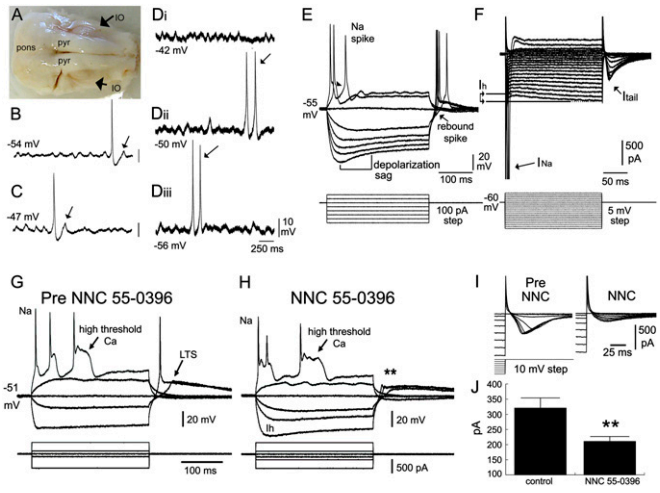

Fig. 2. Electrophysiological properties of primate IO neurons. (*A*) Ventral surface of the monkey brainstem. Pyr, pyramidal tracts. (*B* and *C*) Voltage records of two IO neurons showing STOs, spontaneous action potentials, and a rebound response following hyperpolarization (arrow). (*Di–iii*) Another IO neuron (Vrest −50 mV) showing voltage-insensitive STOs as tested by injecting depolarizing (*Di*) and hyperpolarizing (*Diii*) current. Arrows indicate spike doublets at the STO frequency. (*E*) Positive current triggers a sodium spike and an after-depolarizing potential (arrowhead); negative current triggers a depolarization sag; release from hyperpolarization triggers rebound spikes (arrow). (*F*) Currents underlying the sodium spike (I_{Na}), depolarization sag (I_h), and rebound response (I_{tail}). (*G* and *H*) Voltage recordings of an IO neuron before (*G*) and after (*H*) addition of 30 μm NNC 55–0396. (*I*) Current recordings showing that NNC 55–0936 reduced I_{tail}. (*J*) Mean reduction of I_{tail} by NNC 55–0396 ($n = 4$). $**P < 0.01$.

membrane potential that were subthreshold for spiking (subthreshold oscillations, STOs) (Fig. 2 *B–D* and Fig. S2). Among the CON neurons, 25 (47%) showed STOs as indicated by visual inspection and by power spectral density analysis. The mean highest frequency of STOs in CON neurons was 5.6 ± 0.8 Hz, and STOs usually were episodic (Fig. S2 *A–C*), although four neurons showed continuous STOs (Fig. 2 *B–D*). When action potentials fired during STOs, they occurred most often on the rising phase of the STO (Fig. 2 *B–D*), and they occasionally evolved into bursts of action potentials at the STO frequency (Fig. 2*D* and Fig. S2 *A* and *B*). Moreover, spontaneous action potentials often were followed by an after-hyperpolarizing potential and a rebound calcium spike as previously identified in rodents (arrows in Fig. 2 *B* and *C*). Depolarization or hyperpolarization with direct current injection did not change the frequency of the STO or the tendency of the STO to entrain spontaneous action potentials (Fig. 2*D*). As demonstrated in rodents, the voltage insensitivity of STOs in IO neurons is supported by electronic coupling (14, 27, 28), and so the properties of primate IO neurons were consistent with their being coupled oscillators. Neither the properties nor the incidence of STOs differed among the experimental groups, although there was a trend toward slower STOs (3.1 ± 1.9 Hz) in CI neurons (Fig. S2).

With depolarizing current, primate IO neurons showed fast sodium spikes and high-threshold calcium spikes, whereas hyperpolarizing current generated a voltage sag characteristic of I_h (Fig. 2*E*). Rebound spikes were triggered reliably by release from 300 ms of hyperpolarizing current, identical to rodent IO neurons (12, 13, 26). The T-type calcium channel antagonist NNC 55–0396 (15–30 μM) (29,30) suppressed rebound spiking without affecting high-threshold calcium potentials or sodium spikes or reducing inward rectification (Fig. 2 *G* and *H*; $n = 4$). Thus, as in rodents, primate IO rebound spiking required T-type channels.

The currents underlying rebound spiking in IO neurons were characterized with voltage clamping (Fig. 2*F*). Hyperpolarizing voltage steps (from a holding potential of −60 mV) elicited clear inward-rectifying currents mediated by I_h (138 ± 11 pA in response to a 200-ms voltage step to −125 mV; $n = 53$). Stepping from a hyperpolarized membrane potential to −60 mV generated a prominent tail current (I_{tail}) (Fig. 2*F*). Averaged over five hyperpolarizing steps (−70 to −50 mV) NNC 55–0396 reduced I_{tail} from 321 ± 32 to 211 ± 15 pA [$F(1,19) = 17.5$, $P < 0.01$; Fig. 2 *I* and *J*], indicating that I_T contributed significantly to I_{tail} in monkey IO neurons.

To inform experiments on the acute and chronic effects of ethanol on the currents underlying the rebound excitability of IO neurons, we performed pharmacological experiments to determine the contributions of the slow deactivation of I_h (31) and the activation of I_T to I_{tail} (Fig. S3). We used mouse IO neurons, which were more conveniently available for highly detailed pharmacology. ZD-7288 (10–20 μM), an antagonist of HCN channels (32, 33), completely blocked I_h during hyperpolarizing voltage steps (Fig. S3 *A* and *B*) and reduced mean I_{tail} by 47% ($n = 8$). A recent report (34) indicated that 10–20 μM ZD-7288 can act nonspecifically to block ∼20% of I_T, independent of its effect on I_h, suggesting a 27% contribution of I_h to I_{tail} in IO neurons. The converse experiment demonstrated that NNC 55-0396 (100 μM) did not affect I_h but reduced mean I_{tail} by 76% (Fig. S3 *C* and *D*), to suggest that a current other than I_T contributed 24% to I_{tail}. To check the pharmacology, we calculated the maximum contribution of I_h to I_{tail} using the modified Goldman-Hodgkin-Katz equation (GHK) and published characteristics of I_h (ref. 35 and *SI Methods*). GHK estimated the maximum contribution of I_h to I_{tail} to be 15%, close to the estimate derived from pharmacology. To verify that the relationship between I_h and I_{tail} was similar between species, we compared variations in I_h vs. I_{tail} (Fig. S4). Linear regression derived nearly identical slopes, indicating that I_h contributed similarly to I_{tail} in mouse and monkey. This allowed us to average the pharmacology and biophysical estimates to conclude that the deactivation of I_h can contribute ∼20% to I_{tail}.

Ethanol Acutely Inhibits I_{tail} by Inhibiting I_T. The sensitivity of IO neurons to ethanol was tested by exposing IO neurons taken from four CON monkeys to 10 and 100 mM ethanol, bracketing the concentrations measured from the BECs (10–60 mM). Ten mM lies within the concentration range (7–19 mM) that contains the threshold for ethanol to inhibit olivocerebellar activity in vivo (36). Ethanol decreased the magnitude of I_{tail} in a concentration-dependent manner ($F(2,59) = 7.2$, $P < 0.01$; Fig. 3 *A* and *B*). To determine whether ethanol reduced I_{tail} by inhibiting I_T, by inhibiting I_h, or both, we performed experiments in mouse IO neurons in the presence of specific channel blockers. Block of I_h by ZD-7288 isolated the I_T component of I_{tail} (Fig. S5*A*). Subsequent application of 100 mM ethanol reduced I_T by 60% (Fig. S5 *A* and *B*). The complementary experiment indicated that ethanol did not inhibit I_{tail} by inhibiting I_h. Block of I_T by NNC 55-0396 unmasked the I_h component of I_{tail} (Fig. S5*C*), which was not inhibited by ethanol (Fig. S5 *C* and *D*). Thus, the inhibition of I_{tail} by ethanol was due to inhibition of I_T.

Ethanol's inhibition of I_T was not due to an effect on the voltage dependence of inactivation (Fig. S6*A*). Conversely, ethanol significantly enhanced the rate of I_T deinactivation. To study deinactivation, we varied the duration of a 50-mV hyperpolarizing step from 50 to 750 ms (Fig. S6*B*) (37, 38). $Ca_V3.1$ channels are largely inactive at resting potential and recover from inactivation in both a time- and voltage-dependent manner. Both 10 and 100 mM ethanol accelerated the recovery from inactivation, similar to the effect of long-chain alcohols (20). Because the voltage-dependence of inactivation was not affected and the deinactivation kinetics were not slowed, the decrease in I_T must have been due to a decrease in conductance and/or number of available channels. Conversely, ethanol potentiated I_h in a concentration-dependent manner ($F(2,67) = 5.4$, $P < 0.01$; Fig. 3 *C* and *D*) without affecting its voltage-dependence of activation (Fig. S6*E*). The consequence of ethanol's inhibiting I_T was to reduce rebound firing (Fig. S6*D*). We next studied alcoholic primates.

Ethanol Washout After Chronic Intoxication Reveals Hyperexcitable Rebound Firing That Is Reversed by Sustained Abstinence. Among the IO neurons studied, there were no differences among the drinking groups in resting potential (CON −51.0 ± 1; CI −52.4 ± 1; RSA −49.4 ± 1 mV) or input resistance (CON 263 ± 18; CI 217 ± 25; RSA

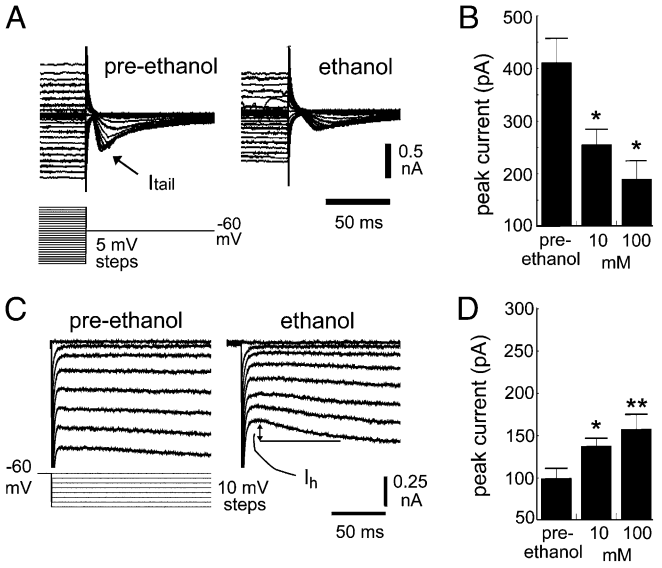

Fig. 3. Acute effect of ethanol on pacemaking currents in primate IO neurons. (*A*) Inactivation protocol to study I_{tail}. One hundred millimoles of ethanol reduced peak I_{tail} in response to a range of voltage steps to −60 mV. (*B*) Effect of 10 and 100 mM ethanol on peak values of Itail (*P <0.05 compared with preethanol). (*C*) Protocol for testing effect of ethanol on I_h showing a robust augmentation of I_h by 100 mM ethanol. (*D*) Effect of 10 and 100 mM ethanol on peak values of I_h (*$P < 0.05$; **$P < 0.01$ compared to preethanol).

237 ± 12 MΩ). In current clamping, the voltage and time dependence of rebound firing were tested by varying the magnitude and duration of hyperpolarization steps (Fig. 4). In a representative IO neuron from a CON monkey, increasing the magnitude or duration of negative current injection increased the probability of a rebound spike upon release from hyperpolarization (Fig. 4*A*). Fig. 4 *B* and *C* shows representative neurons taken from CI and RSA monkeys. In comparison with the CON neuron, the CI neuron required less hyperpolarizing current to elicit a rebound spike large enough to trigger an action potential. The hyperexcitability seen in the CI neuron was not seen in the neuron from the RSA monkey, suggesting its reversal by abstinence.

Average plots of rebound excitability demonstrated a significant increase in the excitability of 17 IO neurons from CI monkeys during acute ethanol washout, so that briefer and smaller hyperpolarizing steps triggered a rebound spike (Fig. 4 *D* and *E*). The hyperexcitability was not present in 48 neurons from RSA monkeys, and, in fact, RSA neurons were less excitable than CON neurons to hyperpolarization (Fig. 4 *D* and *F*).

To present the excitability changes induced by chronic ethanol intoxication more easily, we plotted the probability of rebound firing as a function of hyperpolarization strength (the product of the duration and magnitude of the injected current). The probability of rebound firing in CON neurons showed a linear relationship to hyperpolarization strength on a semilog graph (Fig. 4*G*). ANOVA indicated a significant main effect of group [$F(2,115) = 4.6$, $P < 0.05$]. Follow-up tests indicated that the excitability of both CI and RSA neurons deviated from CON neurons for hyperpolarizations >60 nA*ms, with CI neurons becoming hyperexcitable and RSA neurons becoming hypoexcitable ($P < 0.05$).

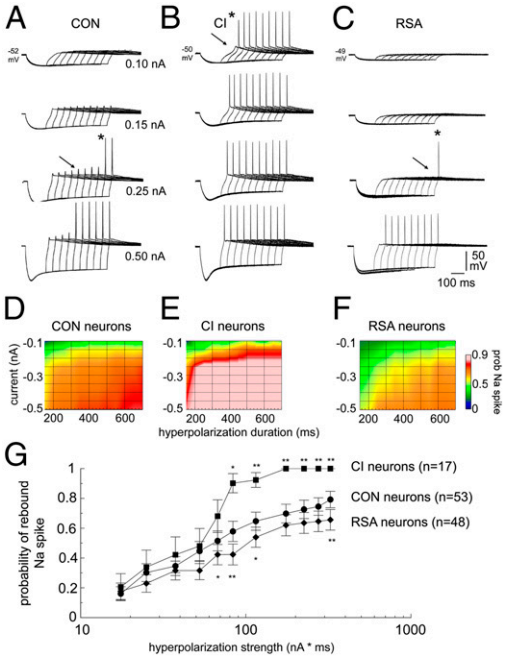

Fig. 4. Changes in the voltage and time dependence of rebound firing with chronic ethanol intoxication and repeated abstinences in IO neurons. (*A–C*) Voltage responses triggered by hyperpolarizing current in three neurons from CON (*A*), CI (*B*), and RSA (*C*) monkeys. Responses were triggered by injecting four hyperpolarizing currents (0.1–0.5 nA) for increasingly longer durations (150–600 ms). Arrows indicate the threshold for eliciting a low-threshold spike, and asterisks indicate the first occurrence of an action potential. (*D–F*) Voltage dependence and time dependence of spiking for CON ($n = 53$) (*D*), CI ($n = 17$) (*E*), and RSA ($n = 48$) (*F*) neurons. (*G*) Semilog plot of the probability of a rebound spike vs. hyperpolarization strength. *$P < 0.05$; **$P < 0.01$ vs. CON.

Bidirectional Plasticity of Pacemaking Currents Underlies Hyper- and Hypoexcitability of IO Neurons Produced by Chronic Intoxication and Sustained Abstinence. Voltage clamping was used to quantify changes in I_T and I_h and to estimate their relative contributions to the excitability changes reported above. We hypothesized that CI monkeys would show an up-regulation in I_{tail} and that RSA monkeys would show a down-regulation in I_{tail}. Measurements of I_{tail} using a −50-mV step for 150 ms revealed a significant effect of group [$F(2,111) = 7.1$, $P < 0.01$; Fig. 5*A*] with opposite modulations in CI and RSA neurons. In 16 neurons from CI monkeys, peak I_{tail} was increased significantly by 33% to 446 ± 54 pA relative to the values from CON monkeys (336 ± 29 pA; $P < 0.05$). In contrast, peak I_{tail} was decreased by 24% to 256 ± 20 pA ($P < 0.05$) in 46 neurons from RSA monkeys. Mean current traces illustrated the significant augmentation of I_{tail} by acute ethanol washout in CI neurons and the significant reduction in RSA neurons (Fig. 5*B*). Acute washout in CI neurons revealed that long-term intoxication increased the rate at which channels conducting I_{tail} deinactivated to hyperpolarization, consistent with an effect in which $Ca_V3.1$ channels compensate for chronic ethanol by increasing their sensitivity to shorter-duration hyperpolarizing pulses (Fig. 5*C*). The change in deinactivation kinetics was reversed by abstinence.

We hypothesized that chronic ethanol intoxication would induce a homeostatic reduction in I_h as a response to the acute effect of ethanol to augment I_h in primate IO neurons. This hypothesis was not true, because peak values of I_h were unaffected by chronic ethanol as measured in the CI group (138 ± 11 pA vs. 132 ± 25 pA; Fig. 5*D*). However, peak values of I_h were reduced significantly by 41% in neurons obtained from RSA monkeys, to 81 ± 9 pA ($P < 0.01$; Fig. 5*D*). Average current traces (Fig. 5*E*) illustrated the significant reduction of I_h in IO neurons of RSA monkeys without a change in the voltage dependence of activation (Fig. 5*F*).

To estimate the contribution of modulations in I_T to the excitability changes, we deduced values of I_T in IO neurons of each drinking group. Because I_h makes up 20% of I_{tail} under control conditions, we calculated that the mean contribution of I_h to I_{tail} was 67 pA after a 150-ms, −50-mV hyperpolarizing pulse. We calculated the change in the I_h contribution to I_{tail} from the measured percentage changes in I_h during hyperpolarization in each group (0.9% and 39.8% reductions for CI and RSA groups, respectively) and subtracted that value from the measured I_{tail} to deduce each neuron's peak I_T. Deduced values of I_T were 270 ± 24 pA for CON, 380 ± 52 pA for CI, and 216 ± 20 pA for RSA neurons (Fig. 5*G*). Thus, chronic intoxication induced a robust increase in I_T that recovered to the preethanol level with abstinence.

Fig. 5*G* summarizes the adaptations for each monkey in a plot of I_{tail} vs. I_h. Acute washout of ethanol produced a pure rightward shift in CI monkeys, indicating a change in excitability specifically caused by a change in I_T. Sustained abstinence after long-term intoxication produced a leftward and downward shift in RSA monkeys proportionate to a return of I_T to the preethanol value and a compensatory decrease in I_h.

Discussion

The main findings were that long-term ethanol intoxication specifically increased I_T in primate IO neurons, whereas long-term intoxication followed by sustained abstinence restored I_T to the preethanol value but reduced I_h to below the preethanol state as an apparent compensation for the initial change in excitability. The increase in I_T observed during acute ethanol washout produced a state of hyperexcitability in IO neurons that greatly enhanced their probability of rebound firing after hyperpolarization, a mechanism that could account for the tremor that we observed in monkeys in acute withdrawal. In contrast, sustained abstinence produced a significant reduction in I_h that was evident 30 d after the monkey's last drink. Thus, sustained abstinence following long-term intoxication was associated with an enduring change in the excitability of IO neurons. Because the IO plays an important role in regulating cerebellar activity and has been implicated in movement control, learning, and

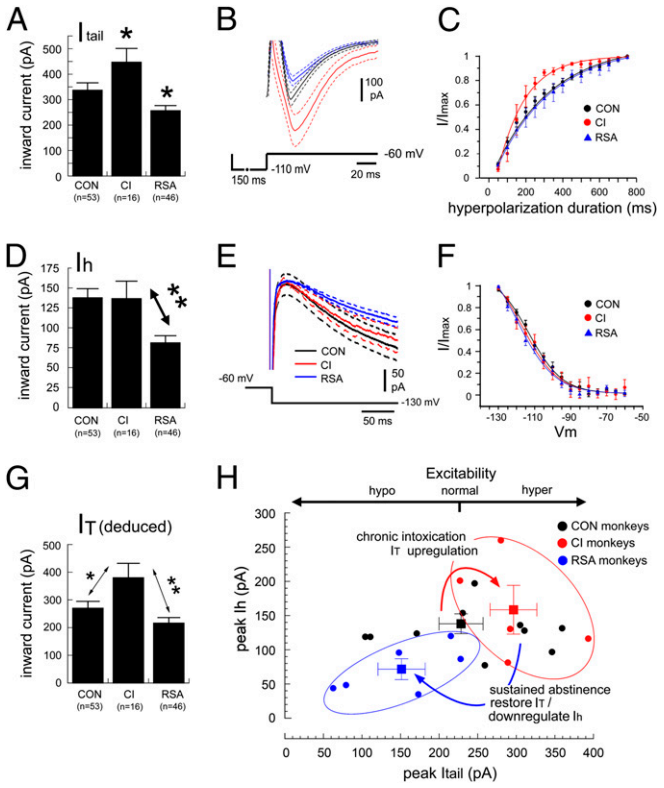

Fig. 5. Bidirectional plasticity of hyperpolarization-activated currents induced by chronic ethanol intoxication and subsequent abstinence. (*A*) Values of peak I_{tail} for the three groups in response to a 50-mV hyperpolarizing step for 150 ms. *$P < 0.05$ vs. CON. (*B*) Mean (±1 SEM) traces of I_{tail} for CON (black), CI (red), and RSA (blue) monkeys. (*C*) Mean I_{tail} deinactivation curves for the three groups fit with exponential functions. τ: CON, 254 ms; CI, 146 ms; RSA, 296 ms. (*D*) Values of peak I_h for the three drinking groups in response to a 65-mV hyperpolarizing step. **$P < 0.01$. (*E*) Mean (±1 SEM) traces of I_h for CON, CI, and RSA neurons. (*F*) Mean I_h activation curves ($V_{1/2}$ and k: CON, −117 mV and 2.2, respectively; CI, −118 mV and 2.3, respectively; RSA, −119 mV and 2.4, respectively). (*G*) Mean values of peak I_T deduced for the three drinking groups. *$P < 0.05$; **$P < 0.01$. (*H*) Bidirectional plasticity of excitability induced by chronic ethanol intake. The excitability of CI monkey IO neurons (red) was enhanced by an up-regulation of I_T without a change in I_h; the excitability of RSA monkey IO neurons (blue) was inhibited by the restoration of I_T to normal and the suppression of I_h. Solid lines represent the mean trace and dotted lines represent 1 SEM from the means. The squares and error bars indicate the mean (±1 SEM) of the groups.

cognition (8, 9), a persistent change in IO function may contribute to long-term neurological impairments in alcoholics. Moreover, the IO is a site for integration of prelimbic and premotor cortical output (39, 40), also indicating that IO dysfunction may underlie aspects of cognitive impairment in alcoholism.

Using IO neurons as a model system, the experiments demonstrated a form of bidirectional plasticity of the intrinsic membrane properties of primate neurons induced by ethanol. The plasticity operates on pacemaking currents involved in the rebound response to hyperpolarization and is in the direction of being homeostatic (41) but is not precisely so. This plasticity was illustrated in the coordinated responses of T-type and HCN channels to ethanol intoxication and abstinence. For T-type channels, the plasticity induced by ethanol was bidirectional. An up-regulation of I_T during chronic intoxication compensated for ethanol's acute effect in suppressing I_T, and the later down-regulation of I_T during abstinence helped restore normal excitability. Although ethanol enhanced I_h acutely, I_h was not down-regulated by chronic intoxication. Nevertheless, I_h was down-regulated during sustained abstinence, a homeostatic response to the overall hyperexcitability unmasked by removing ethanol. The combined down-regulations in I_T and I_h with sustained abstinence persistently depressed excitability.

The adaptation of $Ca_V3.1$ and HCN channels to ethanol is complex. During continuous intoxication, IO neurons adapted to ethanol by increasing the rate at which $Ca_V3.1$ channels were deinactivated and by increasing the magnitude of I_T. $Ca_V3.1$ channels readapted to sustained abstinence by restoring their deinactivation kinetics and reducing the peak current. An interesting finding was the degree to which T-type channels' recovery from inactivation was modifiable by acute and chronic experience with ethanol. Phosphorylation regulates the deinactivation kinetics of $Ca_V3.1$ channels (42) and may contribute to those changes. The acute enhancement of I_h by ethanol in the primate IO was consistent with observations in some rodent neurons (21, 43). However, CI monkeys did not demonstrate a compensatory reduction in I_h. Instead, I_h was down-regulated only by abstinence from ethanol following severe intoxication. The trigger to down-regulate I_h may be the hyperexcitability during withdrawal or may be coupled to a compensatory decrease in I_T independent of the excitability change. The latter mechanism is suggested by a report demonstrating down-regulation of I_h after $Ca_V3.1$ gene deletion (22).

The experiments provide support for plasticity in I_T associated with chronic ethanol intoxication in primates. Using monkeys treated like our CI group, a recent study (44) found plasticity in I_T with chronic ethanol in the lateral geniculate nucleus (LGN). Although the direction of plasticity was opposite to our finding in the IO, low doses of ethanol augmented I_T in LGN neurons (45), and the monkeys in that study (44) consumed less ethanol per day than did our CI group. The different outcomes could be caused by different $Ca_V3.1$ splice variants (46). The changes in excitability after sustained abstinence add to a number of alterations produced by chronic ethanol that persist after acute withdrawal, such as the up-regulation of NMDA receptor activity (47) and aberrant hypothalamo-pituitary-adrenal axis function (48), or that reverse and overshoot the preethanol state, such as for cannabinoid synaptic transmission (49). Key questions are whether the suppressed excitability requires repeated abstinences and can recover and whether the adaptation observed in CI neurons provides resistance to ethanol.

It has been proposed that oscillatory activity of the IO is a fundamental property of vertebrate motor systems to provide temporal and spatial precision to movement and learning (8, 9). A contrasting hypothesis is that the primate IO is nonoscillatory (50). The present experiments support the former hypothesis by providing direct evidence that primate IO neurons contain the same pacemaking currents as rodent IO neurons and that primate IO neurons can generate STOs in membrane potential. Primate STOs often were episodic, as measured in rodents in vivo (51, 52), and their frequency (5.1 Hz) was within the frequency range seen in rodents and deduced on the basis of multielectrode recording in vivo during movement (53). The conservation of those properties through phylogeny suggests a vital role for IO oscillation in sensory–motor integration.

With regard to alcoholism, our findings indicate that long-term intoxication and repeated withdrawals produce a persistent alteration of the intrinsic electrical excitability of IO neurons. Excessive bidirectional plasticity of $Ca_V3.1$ and HCN channels in the IO and elsewhere may contribute to the persistent neurological consequences of chronic alcoholism and relapse, and its mechanisms could be targets for therapy.

Methods

Primate Procedures. Primate procedures were approved by the Oregon National Primate Research Center Animal Care and Use Committee and carried out according to the National Institutes of Health Guidelines for the Care and Use of Mammals in Neuroscience and Behavioral Research. The procedures are described in detail in *SI Methods*. Cynomolgus monkeys were induced to drink up to 1.5 $g \cdot kg^{-1} \cdot d^{-1}$ of 4% ($w \cdot v^{-1}$) ethanol (diluted with water) by schedule-induced polydipsia in a method previously described (5–7). Thereafter, monkeys were allowed free access to 4% ethanol and water for 22 h/d (11:00 AM to 9:00 AM). The quantity of self-administered ethanol was measured daily by mass displacement. After 1 y of chronic intoxication, CI monkeys were killed and necropsied. RSA monkeys initially self-administered

ethanol as in the protocol for CI monkeys and then were given an additional 4 mo of open access followed by 28 d of abstinence; this sequence was repeated two more times before necropsy.

Brainstem Slice Preparation and Whole-Cell Recording. After ketamine sedation, animals were intubated and maintained on a mixture of 1 L O_2 and room air in order to ensure O_2 saturation. Sodium pentobarbital was given to establish deep anesthesia, during which the calvaria was removed, and the brain with dura intact was exposed. The monkeys then were perfused through the heart with cold, oxygenated artificial cerebrospinal fluid (ACSF). The brain was removed within 5 min after death and was prepared for electrophysiology.

Slices were submerged in a recording chamber perfused with room-temperature ACSF. After a gigaohm seal was established, signals were amplified and digitized. Voltage-clamp recordings were obtained using a holding potential of −60 mV and were discontinued if the leak was >20% of control.

ACKNOWLEDGMENTS. We thank Prof. C. Bell for providing space and Dr. A. Wei for assistance with the Boltzmann functions. We also thank the Oregon National Primate Research Center Surgical and Pathology Units. This work was supported by National Institutes of Health Grants R01 NS31224-17 (to J.P.W.), R01 AA016748 (to J.B.D.), U01 AA013510-10 (to K.A.G.), U01 AA013641-10 (to K.A.G.), and P51 RR00163 (to K.A.G. and J. Robertson).

1. Edwards G, Gross MM (1976) Alcohol dependence: Provisional description of a clinical syndrome. *BMJ* 1:1058–1061.
2. Myrick H, Anton RF (1998) Treatment of alcohol withdrawal. *Alcohol Health Res World* 22:38–43.
3. Harris RA (1999) Ethanol actions on multiple ion channels: Which are important? *Alcohol Clin Exp Res* 23:1563–1570.
4. Yang L, Long C, Evans MS, Faingold C (2002) Ethanol withdrawal results in aberrant membrane properties and synaptic responses in periaqueductal gray neurons associated with seizure susceptibility. *Brain Res* 957:99–108.
5. Grant KA, Bennett AJ (2003) Advances in nonhuman primate alcohol abuse and alcoholism research. *Pharmacol Ther* 100:235–255.
6. Vivian JA, et al. (2001) Induction and maintenance of ethanol self-administration in cynomolgus monkeys (*Macaca fascicularis*): Long-term characterization of sex and individual differences. *Alcohol Clin Exp Res* 25:1087–1097.
7. Grant KA, et al. (2008) Drinking typography established by scheduled induction predicts chronic heavy drinking in a monkey model of ethanol self-administration. *Alcohol Clin Exp Res* 32:1824–1838.
8. Llinás RR (1991) The non-continuous nature of movement execution. *Motor Control: Concepts and Issues*, eds Humphrey DR, Freund H-J (John Wiley & Sons, New York), pp 223–242.
9. Welsh JP, Llinás R (1997) Some organizing principles for the control of movement based on olivocerebellar physiology. *Prog Brain Res* 114:449–461.
10. Deuschl G, Elble RJ (2000) The pathophysiology of essential tremor. *Neurology* 54(11):,Suppl 4):S14–S20.
11. Loewenstein Y (2002) A possible role of olivary gap-junctions in the generation of physiological and pathological tremors. *Mol Psychiatry* 7:129–131.
12. Llinás R, Yarom Y (1981) Electrophysiology of mammalian inferior olivary neurones in vitro. Different types of voltage-dependent ionic conductances. *J Physiol* 315: 549–567.
13. Llinás R, Yarom Y (1981) Properties and distribution of ionic conductances generating electroresponsiveness of mammalian inferior olivary neurones in vitro. *J Physiol* 315: 569–584.
14. Llinás R, Yarom Y (1986) Oscillatory properties of guinea-pig inferior olivary neurones and their pharmacological modulation: An in vitro study. *J Physiol* 376:163–182.
15. Llinás R, Volkind RA (1973) The olivo-cerebellar system: Functional properties as revealed by harmaline-induced tremor. *Exp Brain Res* 18:69–87.
16. Martin FC, Thu Le A, Handforth A (2005) Harmaline-induced tremor as a potential preclinical screening method for essential tremor medications. *Mov Disord* 20:298–305.
17. Bleasel AF, Pettigrew AG (1992) Development and properties of spontaneous oscillations of the membrane potential in inferior olivary neurons in the rat. *Brain Res Dev Brain Res* 65:43–50.
18. Bal T, McCormick DA (1997) Synchronized oscillations in the inferior olive are controlled by the hyperpolarization-activated cation current I(h). *J Neurophysiol* 77:3145–3156.
19. Walter HJ, Messing RO (1999) Regulation of neuronal voltage-gated calcium channels by ethanol. *Neurochem Int* 35:95–101.
20. Eckle VS, Todorovic SM (2010) Mechanisms of inhibition of CaV3.1 T-type calcium current by aliphatic alcohols. *Neuropharmacology* 59:58–69.
21. Okamoto T, Harnett MT, Morikawa H (2006) Hyperpolarization-activated cation current (I_h) is an ethanol target in midbrain dopamine neurons of mice. *J Neurophysiol* 95:619–626.
22. Park YG, et al. (2010) Ca(V)3.1 is a tremor rhythm pacemaker in the inferior olive. *Proc Natl Acad Sci USA* 107:10731–10736.
23. Handforth A, et al. (2010) T-type calcium channel antagonists suppress tremor in two mouse models of essential tremor. *Neuropharmacology* 59:380–387.
24. Placantonakis DG, Bukovsky AA, Zeng XH, Kiem HP, Welsh JP (2004) Fundamental role of inferior olive connexin 36 in muscle coherence during tremor. *Proc Natl Acad Sci USA* 101:7164–7169.
25. Dissanaike S, Halldorsson A, Frezza EE, Griswold J (2006) An ethanol protocol to prevent alcohol withdrawal syndrome. *J Am Coll Surg* 203:186–191.
26. Placantonakis DG, Schwarz C, Welsh JP (2000) Serotonin suppresses subthreshold and suprathreshold oscillatory activity of rat inferior olivary neurones in vitro. *J Physiol* 524:833–851.
27. Long MA, Deans MR, Paul DL, Connors BW (2002) Rhythmicity without synchrony in the electrically uncoupled inferior olive. *J Neurosci* 22:10898–10905.
28. De Zeeuw CI, et al. (2003) Deformation of network connectivity in the inferior olive of connexin 36-deficient mice is compensated by morphological and electrophysiological changes at the single neuron level. *J Neurosci* 23:4700–4711.
29. Huang L, et al. (2004) NNC 55-0396 [(1S,2S)-2-(2-(N-[(3-benzimidazol-2-yl)propyl]-N-methylamino)ethyl)-6-fluoro-1,2,3,4-tetrahydro-1-isopropyl-2-naphtyl cyclopropanecarboxylate dihydrochloride]: A new selective inhibitor of T-type calcium channels. *J Pharmacol Exp Ther* 309:193–199.
30. Li M, Hansen JB, Huang L, Keyser BM, Taylor JT (2005) Towards selective antagonists of T-type calcium channels: Design, characterization and potential applications of NNC 55-0396. *Cardiovasc Drug Rev* 23:173–196.
31. Bal R, Oertel D (2000) Hyperpolarization-activated, mixed-cation current (I(h)) in octopus cells of the mammalian cochlear nucleus. *J Neurophysiol* 84:806–817.
32. BoSmith RE, Briggs I, Sturgess NC (1993) Inhibitory actions of ZENECA ZD7288 on whole-cell hyperpolarization activated inward current (If) in guinea-pig dissociated sinoatrial node cells. *Br J Pharmacol* 110:343–349.
33. Harris NC, Constanti A (1995) Mechanism of block by ZD 7288 of the hyperpolarization-activated inward rectifying current in guinea pig substantia nigra neurons in vitro. *J Neurophysiol* 74:2366–2378.
34. Sánchez-Alonso JL, Halliwell JV, Colino A (2008) ZD 7288 inhibits T-type calcium current in rat hippocampal pyramidal cells. *Neurosci Lett* 439:275–280.
35. Aponte Y, Lien C-C, Reisinger E, Jonas P (2006) Hyperpolarization-activated cation channels in fast-spiking interneurons of rat hippocampus. *J Physiol* 574:229–243.
36. Servais L, et al. (2005) Effect of chronic ethanol ingestion on Purkinje and Golgi cell firing in vivo and on motor coordination in mice. *Brain Res* 1055:171–179.
37. Coulter DA, Huguenard JR, Prince DA (1989) Calcium currents in rat thalamocortical relay neurones: Kinetic properties of the transient, low-threshold current. *J Physiol* 414:587–604.
38. Hering J, Feltz A, Lambert RC (2004) Slow inactivation of the Ca(V)3.1 isotype of T-type calcium channels. *J Physiol* 555:331–344.
39. Watson TC, Jones MW, Apps R (2009) Electrophysiological mapping of novel prefrontal - cerebellar pathways. *Front Integr Neurosci* 3:1–11.
40. Dias-Ferreira E, Sousa N, Costa RM (2010) Frontocerebellar connectivity: Climbing through the inferior olive. *Front Neurosci* 4:1–2.
41. Marder E, Goaillard J-M (2006) Variability, compensation and homeostasis in neuron and network function. *Nat Rev Neurosci* 7:563–574.
42. Leresche N, Hering J, Lambert RC (2004) Paradoxical potentiation of neuronal T-type Ca^{2+} current by ATP at resting membrane potential. *J Neurosci* 24:5592–5602.
43. Yan H, et al. (2009) Developmental sensitivity of hippocampal interneurons to ethanol: Involvement of the hyperpolarization-activated current, Ih. *J Neurophysiol* 101:67–83.
44. Carden WB, et al. (2006) Chronic ethanol drinking reduces native T-type calcium current in the thalamus of nonhuman primates. *Brain Res* 1089:92–100.
45. Mu J, Carden WB, Kurukulasuriya NC, Alexander GM, Godwin DW (2003) Ethanol influences on native T-type calcium current in thalamic sleep circuitry. *J Pharmacol Exp Ther* 307:197–204.
46. Monteil A, et al. (2000) Molecular and functional properties of the human alpha(1G) subunit that forms T-type calcium channels. *J Biol Chem* 275:6090–6100.
47. Wang J, et al. (2010) Long-lasting adaptations of the NR2B-containing NMDA receptors in the dorsomedial striatum play a crucial role in alcohol consumption and relapse. *J Neurosci* 30:10187–10198.
48. Rasmussen DD, et al. (2000) Chronic daily ethanol and withdrawal: 1. Long-term changes in the hypothalamo-pituitary-adrenal axis. *Alcohol Clin Exp Res* 24: 1836–1849.
49. Mitrirattanakul S, et al. (2007) Bidirectional alterations of hippocampal cannabinoid 1 receptors and their endogenous ligands in a rat model of alcohol withdrawal and dependence. *Alcohol Clin Exp Res* 31:855–867.
50. Keating JG, Thach WT (1995) Nonclock behavior of inferior olive neurons: Interspike interval of Purkinje cell complex spike discharge in the awake behaving monkey is random. *J Neurophysiol* 73:1329–1340.
51. Khosrovani S, Van Der Giessen RS, De Zeeuw CI, De Jeu MTG (2007) In vivo mouse inferior olive neurons exhibit heterogeneous subthreshold oscillations and spiking patterns. *Proc Natl Acad Sci USA* 104:15911–15916.
52. Chorev E, Yarom Y, Lampl I (2007) Rhythmic episodes of subthreshold membrane potential oscillations in the rat inferior olive nuclei *in vivo*. *J Neurosci* 27:5043–5052.
53. Welsh JP, Lang EJ, Suglhara I, Llinás R (1995) Dynamic organization of motor control within the olivocerebellar system. *Nature* 374:453–457.